Published in final edited form as:
Cell Host Microbe. 2013 May 15; 13(5): 521–534. doi:10.1016/j.chom.2013.04.009.

Malaria infected erythrocyte-derived microvesicles mediate cellular communication within the parasite population and with the host immune system

Pierre-Yves Mantel[1], **Anh N. Hoang**[2,*], **Ilana Goldowitz**[1,*], **Daria Potashnikova**[3,4,*], **Bashar Hamza**[2], **Ivan Vorobjev**[3,5], **Ionita Ghiran**[6], **Mehmet Toner**[2], **Daniel Irimia**[2], **Alexander R. Ivanov**[7], **Natasha Barteneva**[3,8], and **Matthias Marti**[1]

[1]Department of Immunology and Infectious Diseases, Harvard School of Public Health, 665 Huntington Avenue, Boston, MA 02115

[2]BioMEMS Resource Center, Massachusetts General Hospital, 114 16[th]Street, Charlestown, MA 02129, USA

[3]Program in Cellular and Molecular Medicine, Children's Hospital Boston

[4]Department of Cell Biology and Histology, Moscow State University, Moscow 119991, Russia

[5]A.N.Belozersky Institute for Physico-Chemical Biology, Moscow State University, Moscow 119991, Russia

[6]Beth Israel Deaconess Medical Center, 3 Blackfan Circle, Boston, MA 02115, USA

[7]Barnett Institute of Chemical and Biological Analysis, Northeastern University, 360 Huntington Avenue, 412 TF, Boston, MA, 02115, USA

[8]Department of Pediatrics, Harvard Medical School, 200 Longwood Avenue, Boston, MA 02115, USA

Summary

Humans and mice infected with different *Plasmodium* strains are known to produce microvesicles derived from the infected red blood cells (RBC), denoted RMVs. Studies in mice have shown that RMVs are elevated during infection and have pro-inflammatory activity. Here we present a detailed characterization of RMV composition and function in the human malaria parasite *Plasmodium falciparum*. Proteomics profiling revealed the enrichment of multiple host and parasite proteins, in particular of parasite antigens associated with host cell membranes and proteins involved in parasite invasion into RBCs. RMVs are quantitatively released during the asexual parasite cycle prior to parasite egress. RMVs demonstrate potent immunomodulatory properties on human primary macrophages and neutrophils. Additionally, RMVs are internalized by infected red blood cells and stimulate production of transmission stage parasites in a dose-dependent manner. Thus, RMVs mediate cellular communication within the parasite population and with the host innate immune system.

Contact: Matthias Marti (mmarti@hsph.harvard.edu).
*These authors contributed equally to this work

Introduction

Plasmodium falciparum causes more than 200 million cases of malaria and more than 1 million deaths each year (Snow et al., 2005). Rapid asexual amplification of parasites in human red blood cells (RBCs) can result in severe and life-threatening disease, while development of sexual stages or gametocytes is required for successful parasite transmission to the mosquito vector. Here we show that microvesicles are quantitatively released by parasite-infected RBCs and transferred between parasites, regulating the production of malaria transmission stages.

Microvesicles (MVs) are small vesicles (0.1 – 1 μm in size) that are produced by direct plasma membrane blebbing. MVs can contain proteins, RNA and even organelles and act as messengers between cells (Skog et al., 2008). In mammalian cells, the rate of MV release is usually low but can be increased by cell activation or apoptosis. Increased MV production by human cells has been observed in a variety of conditions including cardiovascular disease, arthritis and thalassemia, and tumour cells can constitutively shed a large number of MVs (Cocucci et al., 2009)..

In recent studies malaria patients infected with either *P. falciparum* or the related human parasite *P. vivax* showed elevated levels of MVs derived from platelets and RBCs (Campos et al., 2010; Nantakomol et al., 2011). MV numbers were increased in patients suffering from severe disease and correlated with peripheral blood parasitemia. After antimalarial treatment, the level of MVs decreased rapidly and continued to decrease further between days 3 and 14 (Nantakomol et al., 2011). Flow assays using antibodies against the parasite antigen RESA, which is localized underneath the infected RBC (iRBC) membrane, have suggested that this protein is present in MVs from malaria patients (Nantakomol et al., 2011). Studies in the rodent malaria model (*P. berghei*) have provided evidence that MVs derived from RBCs (RMVs) induce host inflammatory responses and contribute to pathology during malaria infection. These studies have shown that RMVs are elevated during infection and that they have a potent, Toll-like receptor-mediated pro-inflammatory effect on macrophages (Couper et al., 2010).

Here we demonstrate that RMVs are quantitatively released from iRBCs during development of the human malaria parasite *P. falciparum*. The majority of RMVs are released very late in the asexual cycle and they contain both human- and *P. falciparum*-derived proteins and other cargo. We provide evidence that RMVs are both immunostimulatory and act as messengers between iRBCs. RMVs are transferred among iRBCs and alter the production of transmission stages within a population. Our studies provide a rationale for systematic investigation of the role of RMVs in malaria pathogenesis and as a mediator of cell-cell communication during the parasite life cycle.

Results

RMVs are released from RBC *in vitro* cultures infected with *P. falciparum*

To characterize the biogenesis, composition and cellular targets of RMVs in the human malaria parasite *P. falciparum*, we used an *in vitro* model in human RBCs. Imaging flow cytometry analysis revealed that a large number of particles present in cell suspension are smaller than RBCs. Microscopic inspection of individual objects clearly supported cytometric classification into three distinct populations based on size differences: clusters of RBCs (“rosettes”, gate M in Figure 1A), single red blood cells and ghosts (S, probably also containing debris) and small particles that looked like vesicles in the corresponding bright field images (RMV, shown in yellow in Figure 1A).

We developed a protocol for the purification of RMVs from culture supernatant (i.e., what is also referred to as parasite conditioned medium) based on differential centrifugation, filtration and a 60% sucrose cushion (Figure S1A). The protocol was optimized by analysing samples from individual purification steps using imaging flow cytometry analysis, microscopy and western blot. Digestive vacuoles and merozoites were collected in the 3600 g pellet as demonstrated by Giemsa staining and western blot. The 10000 g pellet mostly contains membrane debris as suggested by the presence of spectrin and the absence of hemoglobin. The final RMV pellet is enriched in stomatin and hemoglobin (Figure S1B), and imaging flow cytometry analysis of this fraction demonstrated that the purification procedure resulted in enrichment of vesicles to > 95% of all detected events (Figure 1A). To further confirm the vesicular nature of these objects we stained them with calcein-AM and annexin V. (Figure 1B). Calcein-AM is a membrane-permeable MV marker that becomes fluorescent and trapped in the cytosol upon cleavage by esterases. RMV labelling with calcein-AM dye demonstrated that > 65% of events in the final fraction are positive, suggesting presence of esterase activity within RMVs. Co-labelling with annexin V confirmed the vesicular nature by binding to phosphatidyl serine on the RMV surface.

The final fraction of purified RMVs was analysed by transmission electron microscopy, demonstrating vesicular shape and size in the range between 100 – 400 nm (Figure 1C). We directly observed the release of RMVs from infected red blood cells during time-lapse imaging experiments in which live parasite cultures were imaged every two minutes over two hours (Figure 1D and Movies S1). Imaging revealed that multiple vesicles at different stages of formation exist simultaneously in single iRBCs, suggesting significant RMV production during at least some parts of the parasite cycle.

RMVs from infected RBCs contain parasite material

To characterize the properties and function of RMVs we first purified vesicles from four *P. falciparum* strains and investigated their protein content by separation of samples on an SDS-PAGE gel followed by Coomassie staining (Figure 2A). We observed a similar protein pattern across RMV fractions derived from all parasite strains, which differed from those of uninfected control samples and from isolated parasite schizont stages (Figure 2A).

To detect potential parasite proteins on RMVs, we tested pools of immune sera from malaria patients for reactivity with the same set of samples (Figure 3A). The sera were previously collected from adults in two highly endemic areas in Uganda and Tanzania, as part of the Millennium Village project. Both serum pools strongly reacted with multiple proteins in the infected RMV samples from all parasite strains analysed, but not with any preparation from uninfected RBCs (uRBCs, Figure 2B). The pattern of reactive bands in RMVs was also different from those present in the schizont preparation. Together, these data suggest that RMVs have a distinct composition, and that those derived from iRBCs additionally contain a specific set of parasite antigens.

Proteomic profiling reveals RMVs are enriched in membrane-associated parasite antigens

To identify the parasite and host proteins present in RMVs, we characterized purified RMV samples using mass spectrometry-based proteomic profiling. We analysed RMVs derived from two culture-adapted parasite strains (3D7 and CS2), and from uRBCs as a control. In all the three preparations, we found that the most abundant RBC proteins were components of RBC lipid rafts such as stomatin and band 3, as well as several carbonic anhydrases (Figure 3A and table S2), which are known to be enriched in MVs derived from RBCs (Rubin et al., 2008). To determine whether RMVs are enriched in particular classes of proteins we stratified the hits from the proteomic analysis by GO (gene ontology) localization term enrichment analysis. This analysis revealed that extracellular- and vesicle-

associated moieties are the most enriched in RMVs. By both total absolute peptide counts and GO localization there was no apparent difference in RBC protein content between infected and uninfected RMVs (Figures 3A and S2).

We identified more than 30 parasite proteins in the RMV preparations from 3D7 and CS2 parasite strains (Figure 3B and table S1). These proteins mainly belong to two classes: proteins associated with RBC membranes and proteins involved in parasite invasion into RBCs (Figure 3C). The first class is represented by components of the Maurer's clefts (SBP1, Rex1/2, MAHRP1/2, PfMC-2TM), proteins linked to the RBC surface membrane (Clag3.1/2, RESA and MESA), and proteins associated with the parasitophorous vacuole membrane (PVM; Exp-2, Etramp2). The second class is represented by erythrocyte binding antigens (EBA-175 and EBA-181, which bind to glycophorins during merozoite invasion before being shed) and rhoptry proteins (RhopH2/H3 and Rap2).

To further corroborate the enrichment of some of the proteins found in RMVs, we performed immunoblots of RMV samples using specific antibodies (Figure 3D). These experiments confirmed enrichment of stomatin and partial depletion of spectrin as well as presence of the secreted parasite proteins RESA, SBP1, and at relatively lower abundance the PVM marker Exp-1. Importantly, we did not identify any markers for components of the parasite-induced knob complex on the iRBC surface, including KAHRP and PfEMP1, or resident parasite proteins such as the ER marker BIP. Together with the presence of RBC lipid raft proteins on RMVs, this finding implies that RMVs arise by blebbing from specific sub-domains within the RBC membrane. We also consistently detected the same parasite markers across the two genetically diverse reference parasite strains 3D7 and CS2, suggesting that the composition of RMVs is conserved in *P. falciparum*.

To determine the distribution and orientation of host and parasite proteins within RMVs we performed enzyme protection assays with purified RMVs. RMVs were treated with the detergent Triton X-100 (TX-100) and with either trypsin or Proteinase K. These experiments demonstrated that glycophorin C is present on the RMV surface, as can be expected if RMVs bleb off the RBC surface. We found that stomatin and two parasite proteins, Exp-1 and SBP1, were protected (Figure 3E). It has been previously shown that the C-terminal tail of the Maurer's cleft protein SBP1 faces the RBC cytoplasm while the N-terminus is located in the lumen (Blisnick et al., 2000). The absence of any processed product in our protection assays therefore suggests that the Maurer's cleft membrane is present within the RMV, and it independently confirms RMV integrity in the preparation. We also observed that EBA-175 and EBA-181, two of the most abundant parasite proteins identified by RMV proteomics, are efficiently digested by both trypsin and proteinase K even in the absence of TX-100. This demonstrates that the proteins are only peripherally associated with RMVs upon shedding. The large immunogenic EBA ectodomains face the inside of the microneme and would therefore be protected from enzyme digestion in the case of microneme contamination in our preparation. In conclusion, proteomic profiling demonstrates that RMVs from iRBCs contain i) a set of enriched RBC proteins, and ii) parasite antigens derived from the RBC surface and internalized membranes, in particular from the Maurer's clefts.

Size and density differentiate RMVs from other RBC-derived material

In other systems, microvesicles have been defined as vesicular particles with a specific density in sucrose gradients and a size range from 0.1 to 1 μm (Muralidharan-Chari et al., 2010). To determine whether our preparations from iRBCs and RBCs represent homogenous populations of microvesicles we prepared culture supernatants by ultracentrifugation and layered pellets on a continuous linear sucrose gradient. We obtained ten fractions and analysed them for protein content by BCA and western blot analysis, using the subset of

parasite and host markers described above. We demonstrated that both protein content and specific RMV markers peaked in fractions 3 and 4 (Figure 4A/B). These fractions represent a density of 1.221-1.198 g/cm^3, which is within the range of densities for MV preparations from other cell types and is higher than exosome density (1.08–1.22 g/cm^3)(Raposo et al., 1996). Probing with the merozoite marker AMA-1 was negative, again confirming absence of merozoites and homogeneity of the vesicular population in the preparations. Immunoblotting demonstrated the presence of the putative resident RMV proteins EXP-1, RESA and SBP-1, as well as stomatin and band3 in fractions 3 to 5. To independently confirm particle abundance across the sucrose fractions, and to determine whether RMVs were also homogenous in size, we analyzed RMVs using a nanoparticle tracking technology (NanoSight), which quantifies particles between 0.1 and 1 μm. This analysis confirmed that RMVs peak in sucrose fractions 3 and 4 in preparations from both RBCs and iRBCs, with the majority of RMVs between 100–150 nm in size. The iRBC preparation showed a longer tail in the size distribution, suggesting existence of an additional subset of RMVs with slightly larger size, between 150–250 nm, but with the same density. A similar size distribution was obtained by flow cytometry using size beads and calcein-AM staining (data not shown).

RMV release peaks during schizogony but before parasite egress

To determine whether vesicles are constitutively released, or whether their release is linked to a particular phase in the parasite cycle, we performed a series of kinetic experiments. We collected supernatants from highly synchronized parasite cultures every 12 hours starting at the ring stage and isolated vesicles for total particle quantification by size (using NanoSight), protein content (using BCA) and protein composition (using western blot analysis). These analyses suggested that RMV release increases steadily during the parasite cycle and peaks late during schizogony or shortly thereafter. This dynamic of release coincided with the emergence of a prominent vesicular subpopulation of 150–250 nm in the iRBC preparation only. Immunoblotting revealed concomitant peak levels of parasite RMV markers such as RESA and SBP1 as well as the host markers spectrin and band3 in the vesicular fraction from late schizogony (Figure 5A).

To further distinguish between vesicle release during parasite development or during egress, which can include release of parasite-derived organelles, we used two complementary approaches to either genetically or chemically inhibit parasite egress. It was recently shown that conditional knock-down of the *P. falciparum* calcium-dependent protein kinase 5 (PfCDPK5) results in a block of parasite egress (Dvorin et al., 2010). Using this conditional knock-down line, we collected supernatants and analysed vesicle production over time in the presence or absence of CDPK5 protein. Our results strongly suggest that RMVs are released before and not during parasite egress (Figure 5B). Importantly, similar experiments using the cysteine protease inhibitor e64, an inhibitor of parasite egress (Millholland et al., 2011), could phenocopy this effect (Figure 5B). Altogether these data demonstrate that the peak release of RMVs from iRBCs occurs shortly before egress (i.e., within the last 6–8 hours of the parasite asexual cycle). RMVs are therefore distinct from recently described post-rupture vesicles that are released upon egress of parasites from the red blood cell (Millholland et al., 2011). This conclusion is supported by the absence of markers for these post-rupture vesicles such as the parasite antigens Sera-5 and Sera-6 in RMVs by proteomics (Table S1).

To quantify RMV release from iRBCs and RBCs, we designed an experiment using two lipophilic membrane dyes, which are readily incorporated into RBCs: PKH26, which emits red light, and PKH67, which emits green light. This combination of dyes allows tracking of distinct particle or cell populations. We labelled highly synchronized trophozoite stage iRBCs with PKH67 and mixed them with uRBCs that we labelled with PKH26. Using flow cytometry and fluorescence microscopy, we monitored release of red and green RMVs

during the remainder of the parasite cycle and after reinvasion, in the presence or absence of e64, (see Figure 5C, panel I, for experimental set up). Using different mixtures of labelled iRBCs and RBCs we determined the relative contribution of iRBC-derived RMVs to total RMV production. This demonstrated that iRBCs release about 10 times more RMVs than uRBCs, and e64 experiments independently confirmed that these RMVs are released before egress (Figures 5C and S3).

RMVs derived from iRBCs activate host monocytes and neutrophils

So far we have provided a thorough examination of the composition, biophysical properties and release kinetics of RMVs. In the next series of experiments we aimed to examine their potential physiological role(s). Recent studies in the rodent malaria model have demonstrated that RMVs derived from *P. berghei* iRBCs strongly activate the innate immune response through macrophage stimulation, suggesting a role of iRMVs in malaria pathology (Couper et al., 2010). To investigate the potential of *Plasmodium falciparum* RMVs to modulate the innate immune response in human malaria, we analyzed their effect on human peripheral blood mononuclear cells (PBMCs), macrophages and neutrophils derived from healthy, malaria naive donors.

PBMCs were incubated with RMVs from uninfected and infected RBCs to determine which cell type was activated and whether pro- or anti-inflammatory cytokines were induced. We measured cell markers CD3 (T cells), CD19 (B cells) and CD14 (monocytes) in combination with the activation markers CD54, CD25, CD40 CD163, CD86 and CD36 by flow cytometry; cell viability was assessed by annexin V and propidium iodide staining. These experiments demonstrated that monocytes (CD14+) are the main targets of RMVs (Figures 6A and S4A–C). Specifically, they showed up-regulation of the activation markers CD40, CD54, and CD86 and down-regulation of CD163 upon stimulation with RMVs from iRBCs but not from uRBCs.

To assess the effect of RMVs on human macrophages, monocytes were isolated from PBMCs, differentiated into macrophages and activated with RMVs. qRT-PCR analysis demonstrated that RMVs from iRBCs can activate the pro-inflammatory cytokines IL-6, IL-12 and IL-1β and the anti-inflammatory cytokine IL-10 in a dose-dependent manner (Figure S4D). We confirmed these results on a protein level via ELISA, measuring IL-10 and TNF-α in culture supernatants (Figure 6B). Likewise, qRT-PCR and confirmatory ELISA demonstrated that RMVs induce the expression of IL-10 and TNF-α in PBMCs (Figure S4B/C). Importantly, macrophage activation depends on the active uptake of RMVs, as demonstrated by microscopy of RMV uptake (Figure 6C) and cytokine induction was inhibited in presence of cytochalasin D, an inhibitor of phagocytosis (Figure 6D).

To probe the role of iRBC-derived RMVs on human neutrophils, we incubated freshly isolated human neutrophils with purified RMVs inside a microfluidic device with small migration channels (Butler et al., 2010). Brief exposure (30 min) to RMVs from iRBCs but not from uRBCs activated neutrophils to spontaneously move, even in the absence of any guiding chemotactic gradients (Figure 6E). We also found that neutrophils pre-incubated with RMVs from uRBCs migrated at a slower rate compared those pre-incubated with RMVs from iRBCs or untreated controls. Together these data demonstrate that RMVs from iRBCs but not from uRBCs can strongly stimulate cells of the innate immune system.

RMVs are internalized into iRBCs and induce transmission stage formation

In the PKH experiments described in Figure 5C we noted that in some cases fluorescence from PKH67-labeled vesicles could also be found inside iRBCs suggesting that they had been incorporated into the cell. To further investigate this observation we performed a series

of RMV uptake experiments and phenotypic assays. First we investigated uptake of labeled RMVs by microscopy, immunoelectron microscopy and flow cytometry. Live fluorescence microscopy revealed that PKH67-labeled RMVs are efficiently incorporated into iRBCs, and eventually accumulate in the parasite and at its nuclear periphery (Figure 7A, panel I). Uptake appears to be specific to iRBCs, since RMVs were found mostly bound to the surface of uRBCs (Panel II). Quantification of uptake using PKH67-labeled RMVs also demonstrated that those derived from iRBCs are incorporated at significantly higher rates than those from uRBCs (Figure 7A, panel III). Notably, only a subset of iRBCs internalizes RMVs even at very high concentrations, suggesting that not all iRBCs are equally receptive for uptake. To visualize RMV uptake on an ultrastructural level we performed immune electron microscopy of RBCs after incubation with biotinylated RMVs from infected RBCs. In concordance with live microscopy we observed the presence of labeled vesicles in the host cell cytoplasm and in the parasite (**********Figure 7B). These internalized RMVs are surrounded by additional membranes, suggesting that phagocytosis-like mechanisms are operational in infected RBCs.

To determine whether RMV uptake has a phenotypic effect on parasite growth, we treated ring stage parasites with a serial dilution of purified RMVs and investigated parasitemia after one replication cycle (Figure 7C). While we did not observe a significant alteration in growth rates after 48 hours, we noted the emergence of increased numbers of gametocytes in the parasite culture at later time points. Sexual stages, or gametocytes, are formed from asexual parents at low rates of <0.1–15% per reinvasion round *in vitro. In vivo* gametocyte production appears to cover an equally large range (Alano, 2007). Upon maturation, gametocytes are transmitted to a mosquito vector during a blood meal, where they undergo fertilization and further development. It has been reported that parasite conditioned medium (i.e., the parasite culture supernatants we use for RMV isolation) can increase the proportion of gametocytes formed (Dyer and Day, 2003), and such conditioned medium is commonly used as a stimulus to increase gametocyte production under *in vitro* conditions (Fivelman et al., 2007). The factor(s) responsible for this effect have not yet been identified. To test whether RMVs from conditioned medium have a gametocyte-inducing effect, we quantified gametocyte production in 3D7 parasites upon addition of conditioned medium or purified RMVs derived from the same conditioned medium. These experiments revealed that RMVs derived from iRBCs stimulated increased gametocyte production in a titrable fashion and similar to conditioned medium from late stage parasite cultures, while RMVs from uRBCs had a less pronounced effect and fresh medium produced minimal levels of gametocytes (Figure 7D). Together, these experiments strongly suggest that RMVs from iRBCs are the active component in conditioned medium that stimulates gametocyte production, and that the concentration of these RMVs can regulate gametocyte production on a population level. These observations are in line with the findings presented by Regev-Rudzki et al (Regev-Rudzki et al.).

Discussion

Exosomes and MVs are involved in many physiological processes, and numerous pathological conditions increase their rate of formation. Previous studies have demonstrated that MVs originating from endothelial cells, platelets and RBCs are present during malaria infection and have suggested a link to the host immune response to malaria. In the present study we show that *P. falciparum*-infected RBCs release MVs in a quantitative fashion in the environment. These RMVs contain parasite antigens and are highly immunogenic, stimulating human PBMCs and primary macrophages and activating neutrophil migration. Finally, we provide evidence that RMVs can be internalized by iRBCs and modulate formation of parasite transmission stages. Our studies suggest that RMVs play major roles in the biology of *Plasmodium* parasites and in the pathogenesis of human malaria.

Establishment of a working protocol for RMV isolation from parasite culture supernatant (i.e., conditioned medium) provided us with the opportunity to define RMVs by size, density and composition. Interestingly, within the small fraction of parasite proteins identified in RMVs, proteins resident in the Maurer's clefts are enriched. Maurer's clefts are parasite-induced membrane structures in the host cell that serve as platforms for surface deposition of parasite antigens. We also identified several surface antigens in RMVs; however, RMVs lack components of the knob, a *P. falciparum* cytoadherence complex on the iRBC surface, such as PfEMP1 and KAHRP. This suggests that RMVs are formed from Maurer's cleft structures and from iRBC subregions that exclude knobs. We have also performed a series of complementary experiments to unambiguously demonstrate that RMV release occurs before egress and coincides in timing with the observed disappearance of Maurer's clefts (Gruring et al., 2011). Interestingly, parasites employ host actin to generate a cytoskeleton within the cytoplasm of the iRBC that connects the Maurer's Clefts with the host cell membrane and to which vesicles ranging from 20–200 nm are attached (Cyrklaff et al., 2012). It remains to be demonstrated directly whether these vesicles and RMVs are identical.

Our experiments suggest that production of RMVs from iRBCs is approximately 10-fold higher than from uRBCs within the time frame of the asexual parasite cycle. This confirms data from a recent study suggesting that iRBCs produce roughly 13x more RMVs, both during infection and under *in vitro* conditions, than do uninfected RBCs (Nantakomol et al., 2011). What are the physiological targets of this increased RMV production during malaria infection? We demonstrate that RMVs from iRBCs have potent pro-inflammatory properties. We also demonstrate that macrophages can phagocytose RMVs from iRBCs after opsonization with serum, and that these RMVs strongly induce cytokine release in PBMCs and macrophages. Excessive or deregulated inflammatory responses to malaria, including high levels of TNF-α or inadequate production of regulatory (anti-inflammatory) cytokines such as IL-10 and TGF-β, are associated with the development of cerebral malaria in both human infections and rodent models of disease. Several highly immunogenic parasite factors such as free GPI, hemozoin and DNA are released from parasites and activate the innate host response, however the exact mechanism of their secretion is not known. It remains to be shown whether these factors are indeed present in RMVs and contribute to the observed activation of the host immune system. A local pro-inflammatory response might be beneficiary for the parasite since high levels of inflammatory cytokines are associated with endothelial cell activation and increased sequestration of iRBCs to the microvasculature (Turner et al., 1994). RMVs may also directly interact with and activate endothelial cells to increase receptor expression and therefore increase parasite sequestration. We also show that RMVs from iRBCs strongly activate neutrophils and increase their migration. We hypothesize that this effect may ultimately contribute to the exhaustion of the immune cells observed during malaria.

The second physiological target of RMVs are parasite-infected RBCs. We demonstrate that RMVs from infected RBCs can be internalized by iRBCs and stimulate conversion to the sexual parasite cycle in a titrable fashion. Both RMV uptake and gametocyte formation are positively correlated with RMV density, suggesting that they are functionally linked. This important finding confirms previous trans-well experiments, which demonstrated that an unknown conditioned medium component of no more than 200 nm in size has a stimulating effect on gametocyte formation (Dyer and Day, 2003). It also strongly suggests that malaria parasites sense the RMV concentration in the environment, as a proxy for parasite density, to regulate the trade-off between extending the period of transmissibility (i.e., asexual growth) and increasing commitment to gametocytes. Altogether these observations imply that RMVs are active in cellular communication between parasites and that their uptake may regulate transmission stage production *in vivo*. Density-dependent autoregulation of

proliferation or of coordinated group behavior has been described in both bacteria and unicellular eukaryotes. This autoregulation requires cell-cell communication, and known mechanisms include signal transfer via secreted small molecules or via vesicles. For example, the opportunistic human pathogen *Pseudomonas aeruginosa* packages a small molecule “pseudomonas quinolone signal’ (PQS) in membrane vesicles for delivery to conspecific cells. This allows the cells to sense population density and coordinate activities including production of the secondary metabolite pyocyanin (Mashburn and Whiteley, 2005). Autoregulation of proliferation may be achieved by density-dependent differentiation into non-dividing stages. In the etiological agent of sleeping sickness, *Trypanosoma brucei,* an as yet unidentified stumpy inducing factor (SIF) mediates density sensing and regulates the formation of non-dividing stumpy forms of the parasite, which are required for transmission to the tsetse fly vector (Reuner et al., 1997).

In some systems, a key mechanism by which MVs mediate cellular communication is through micro RNA (miRNA). For example, exchange of miRNAs between antigen-presenting cells and T cells occurs at the site of immune synapses and regulates gene expression in the recipient cells (Mittelbrunn et al., 2011). Endothelial cells secreting miRNA-containing MVs regulate atherosclerosis formation in the aorta by targeting smooth muscle cells (Hergenreider et al., 2012). Although the underlying mechanism by which RMVs influence parasite physiology remains to be determined, the presence of additional membranes surrounding RMVs after transfer into the parasite suggests that intact vesicles are internalized through phagocytosis-like mechanisms. This process may be related to uptake of RBC material through the parasite cytostome, which can deliver vesicles to the parasite food vacuole (Abu Bakar et al., 2010), or to autophagy-related mechanisms. We show that RMVs concentrate around the parasite nucleus. It has recently been demonstrated that parasite-infected sickle cell RBCs produce miRNAs that can translocate into the parasite where they interfere with protein translation and induce formation of gametocytes (LaMonte et al., 2012). We have identified small RNAs including miRNA in RMVs from iRBCs (Figure S5), and it is therefore conceivable that specific miRNA species are also involved in the gametocyte formation phenotype we observed in the internalization experiments. Altogether our study reveals that MVs derived from *P. falciparum*-infected red blood cells possess important functions in immunomodulation and cellular communication. These findings provide a foundation for further investigations into the molecular targets of RMVs and their contents after uptake into infected cells and the implications of this cell-cell communication for the pathology of human malaria.

Experimental Procedures

Experimental procedures are described in further detail in Extended Experimental Procedures.

Preparation of RMVs and other cellular samples

RMVs were isolated by a combination of sequential rounds of centrifugation at increasing speed, high molecular weight cut-off filters and a one step sucrose gradient. Purity of resulting samples was controlled by imaging flow cytometry and western blot analysis of different fractions. Final fractions were further characterized by electron microscopy and a linear sucrose gradient. Detail description of the purification protocol including cellular controls, as well as analysis by imaging flow cytometry, flow cytometry and western blot is included in the extended experimental procedures.

Proteomic profiling of RMVs

Proteomic profiling analyses were performed similarly to what we described previously (Dicker et al., 2010) and as detailed in the Supplementary Material. Isolated MVs were either fractionated by 1D PAGE and then the resulted fractions were in-gel digested (first replicate) or in-solution digested without pre-fractionation (second replicate) prior to nanoLC MS/MS-based proteomic profiling performed in technical duplicates for each digest followed by comparative analysis of identified proteomes and gene ontology terms corresponding to detected proteins. Detailed proteomics procedures and protocols are described in the expanded experimental procedures.

Dynamics of RMV release

Quantitative and temporal dynamics of RMV release across the intra-erythrocytic *P. falciparum* cycle were captured in time course experiments by collecting samples at specific intervals. Chemical and genetic perturbations were used to determine whether RMV release peaks before or during parasite egress. Sample analysis was performed by a combination of western blot and nanoparticle tracking technology (Nanosight). To determine the relative amounts of RMVs released from iRBCs vs uRBCs from within a parasite culture, we also labeled cells with the two lipid dyes PKH26 and PKH67, using flow cytometry as readout. Detailed description of these experiments is available in the extended experimental procedures.

Macrophage and neutrophil activation assays

Macrophage stimulation was assayed using series of activation markers and cytokines, by a combination of qRT-PCR, flow cytometry and ELISA assays. Neutrophil activation was measured microscopically in migration assays within microfluidics devices. Detail procedures are included in the extended experimental procedures.

RMV internalization into iRBCs and phenotypic analysis

Internalization in the presence or absence of inhibitory compounds was done with labeled RMVs and assayed by fluorescence and immunoelectron microscopy as well as flow cytometry. Phenotypic analysis upon RMV incubation was performed in 96-well format using standard assays for parasite growth and gametocyte production (Buchholz et al., 2011). Further details are included in the extended experimental procedures.

Supplementary Material

Refer to Web version on PubMed Central for supplementary material.

Acknowledgments

We acknowledge Maria Ericsson for expert technical support with electron microscopy, and Drs. Barbara Burleigh and Barry Bloom for critical reading of the manuscript. Drs. Klaus Lingelbach (anti-Exp-1), Brian Cooke (anti-SBP1), Diane Taylor (anti-KAHRP), Robin Anders (anti-RESA and anti-AMA1) and Alan Cowman (anti-ATS 6H1, anti-EBA-175 and anti-EBA-181) are gratefully acknowledged for providing specific anti-sera to *P. falciparum* proteins. Anti-BIP has been provided by MR4 as MRA19. Thanks to Drs. Sarah Volkman for parasite strains Sen.T135.09 and Sen.T151.09, Joe Smith for parasite strains Pf2004 and Pf2006, and Manoj Duraisingh for the CDPK5-DD transgenic parasite line. We also acknowledge Dr. Pardis Sabeti for providing us with aliquots of serum samples derived from the Millennium Village Project, and Dr. Barry Karger for his instrumental support. This work has been supported through a collaborative seed grant from Harvard Catalyst to M.M., N.A.B. and A.R.I., a Becton Dickinson Bioscience Immunology Award and NIH grant R21AI105328 (M.M.), a Grand Challenges Exploration Grant OPP1069401 from the Bill and Melinda Gates Foundation (D.I.) and through a Novartis research fellowship to P.-Y.M.

References

Abu Bakar N, Klonis N, Hanssen E, Chan C, Tilley L. Digestive-vacuole genesis and endocytic processes in the early intraerythrocytic stages of Plasmodium falciparum. Journal of cell science. 2010; 123:441–450. [PubMed: 20067995]

Alano P. Plasmodium falciparum gametocytes: still many secrets of a hidden life. Molecular microbiology. 2007; 66:291–302. [PubMed: 17784927]

Blisnick T, Morales Betoulle ME, Barale JC, Uzureau P, Berry L, Desroses S, Fujioka H, Mattei D, Braun Breton C. Pfsbp1, a Maurer's cleft Plasmodium falciparum protein, is associated with the erythrocyte skeleton. Molecular and biochemical parasitology. 2000; 111:107–121. [PubMed: 11087921]

Buchholz K, Burke TA, Williamson KC, Wiegand RC, Wirth DF, Marti M. A high-throughput screen targeting malaria transmission stages opens new avenues for drug development. The Journal of infectious diseases. 2011; 203:1445–1453. [PubMed: 21502082]

Butler KL, Ambravaneswaran V, Agrawal N, Bilodeau M, Toner M, Tompkins RG, Fagan S, Irimia D. Burn injury reduces neutrophil directional migration speed in microfluidic devices. PLoS ONE. 2010; 5:e11921. [PubMed: 20689600]

Campos FM, Franklin BS, Teixeira-Carvalho A, Filho AL, de Paula SC, Fontes CJ, Brito CF, Carvalho LH. Augmented plasma microparticles during acute Plasmodium vivax infection. Malaria journal. 2010; 9:327. [PubMed: 21080932]

Cocucci E, Racchetti G, Meldolesi J. Shedding microvesicles: artefacts no more. Trends Cell Biol. 2009; 19:43–51. [PubMed: 19144520]

Couper KN, Barnes T, Hafalla JC, Combes V, Ryffel B, Secher T, Grau GE, Riley EM, de Souza JB. Parasite-derived plasma microparticles contribute significantly to malaria infection-induced inflammation through potent macrophage stimulation. PLoS pathogens. 2010; 6:e1000744. [PubMed: 20126448]

Cyrklaff M, Sanchez CP, Frischknecht F, Lanzer M. Host actin remodeling and protection from malaria by hemoglobinopathies. Trends in parasitology. 2012

Dicker L, Lin X, Ivanov AR. Increased power for the analysis of label-free LC-MS/MS proteomics data by combining spectral counts and peptide peak attributes. Molecular & cellular proteomics : MCP. 2010; 9:2704–2718.

Dvorin JD, Martyn DC, Patel SD, Grimley JS, Collins CR, Hopp CS, Bright AT, Westenberger S, Winzeler E, Blackman MJ, et al. A plant-like kinase in Plasmodium falciparum regulates parasite egress from erythrocytes. Science. 2010; 328:910–912. [PubMed: 20466936]

Dyer M, Day KP. Regulation of the rate of asexual growth and commitment to sexual development by diffusible factors from in vitro cultures of Plasmodium falciparum. The American journal of tropical medicine and hygiene. 2003; 68:403–409. [PubMed: 12875287]

Fivelman QL, McRobert L, Sharp S, Taylor CJ, Saeed M, Swales CA, Sutherland CJ, Baker DA. Improved synchronous production of Plasmodium falciparum gametocytes in vitro. Molecular and biochemical parasitology. 2007; 154:119–123. [PubMed: 17521751]

Gruring C, Heiber A, Kruse F, Ungefehr J, Gilberger TW, Spielmann T. Development and host cell modifications of Plasmodium falciparum blood stages in four dimensions. Nat Commun. 2011; 2:165. [PubMed: 21266965]

Hergenreider E, Heydt S, Treguer K, Boettger T, Horrevoets AJ, Zeiher AM, Scheffer MP, Frangakis AS, Yin X, Mayr M, et al. Atheroprotective communication between endothelial cells and smooth muscle cells through miRNAs. Nature cell biology. 2012; 14:249–256.

LaMonte G, Philip N, Reardon J, Lacsina JR, Majoros W, Chapman L, Thornburg CD, Telen MJ, Ohler U, Nicchitta CV, et al. Translocation of sickle cell erythrocyte microRNAs into Plasmodium falciparum inhibits parasite translation and contributes to malaria resistance. Cell host & microbe. 2012; 12:187–199. [PubMed: 22901539]

Mashburn LM, Whiteley M. Membrane vesicles traffic signals and facilitate group activities in a prokaryote. Nature. 2005; 437:422–425. [PubMed: 16163359]

Millholland MG, Chandramohanadas R, Pizzarro A, Wehr A, Shi H, Darling C, Lim CT, Greenbaum DC. The malaria parasite progressively dismantles the host erythrocyte cytoskeleton for efficient egress. Molecular & cellular proteomics : MCP. 2011; 10:M111 010678.

Mittelbrunn M, Gutierrez-Vazquez C, Villarroya-Beltri C, Gonzalez S, Sanchez-Cabo F, Gonzalez MA, Bernad A, Sanchez-Madrid F. Unidirectional transfer of microRNA-loaded exosomes from T cells to antigen-presenting cells. Nat Commun. 2011; 2:282. [PubMed: 21505438]

Muralidharan-Chari V, Clancy JW, Sedgwick A, D'Souza-Schorey C. Microvesicles: mediators of extracellular communication during cancer progression. Journal of cell science. 2010; 123:1603–1611. [PubMed: 20445011]

Nantakomol D, Dondorp AM, Krudsood S, Udomsangpetch R, Pattanapanyasat K, Combes V, Grau GE, White NJ, Viriyavejakul P, Day NP, et al. Circulating red cell-derived microparticles in human malaria. The Journal of infectious diseases. 2011; 203:700–706. [PubMed: 21282195]

Raposo G, Nijman HW, Stoorvogel W, Liejendekker R, Harding CV, Melief CJ, Geuze HJ. B lymphocytes secrete antigen-presenting vesicles. The Journal of experimental medicine. 1996; 183:1161–1172. [PubMed: 8642258]

Regev-Rudzki N, Wilson DW, Carvalho TG, Sisquella X, Coleman BM, Rug M, Bursac D, Angrisano F, Gee M, Hill AF, et al. Cell-cell communication between malaria parasites promotes sexual differentiation via exosome-like vesicles. Cell. (*In press*).

Reuner B, Vassella E, Yutzy B, Boshart M. Cell density triggers slender to stumpy differentiation of Trypanosoma brucei bloodstream forms in culture. Molecular and biochemical parasitology. 1997; 90:269–280. [PubMed: 9497048]

Rubin O, Crettaz D, Canellini G, Tissot JD, Lion N. Microparticles in stored red blood cells: an approach using flow cytometry and proteomic tools. Vox Sang. 2008; 95:288–297. [PubMed: 19138258]

Skog J, Wurdinger T, van Rijn S, Meijer DH, Gainche L, Sena-Esteves M, Curry WT Jr, Carter BS, Krichevsky AM, Breakefield XO. Glioblastoma microvesicles transport RNA and proteins that promote tumour growth and provide diagnostic biomarkers. Nat Cell Biol. 2008; 10:1470–1476. [PubMed: 19011622]

Snow RW, Guerra CA, Noor AM, Myint HY, Hay SI. The global distribution of clinical episodes of Plasmodium falciparum malaria. Nature. 2005; 434:214–217. [PubMed: 15759000]

Turner GD, Morrison H, Jones M, Davis TM, Looareesuwan S, Buley ID, Gatter KC, Newbold CI, Pukritayakamee S, Nagachinta B, et al. An immunohistochemical study of the pathology of fatal malaria. Evidence for widespread endothelial activation and a potential role for intercellular adhesion molecule-1 in cerebral sequestration. The American journal of pathology. 1994; 145:1057–1069. [PubMed: 7526692]

Highlights

- Malaria antigens are enriched in microvesicles released from infected RBCs (RMVs)
- RMV release peaks during schizogony but before parasite egress
- RMVs derived from infected RBCs activate host monocytes and neutrophils
- RMVs internalized by infected RBCs stimulate transmission stage parasite development

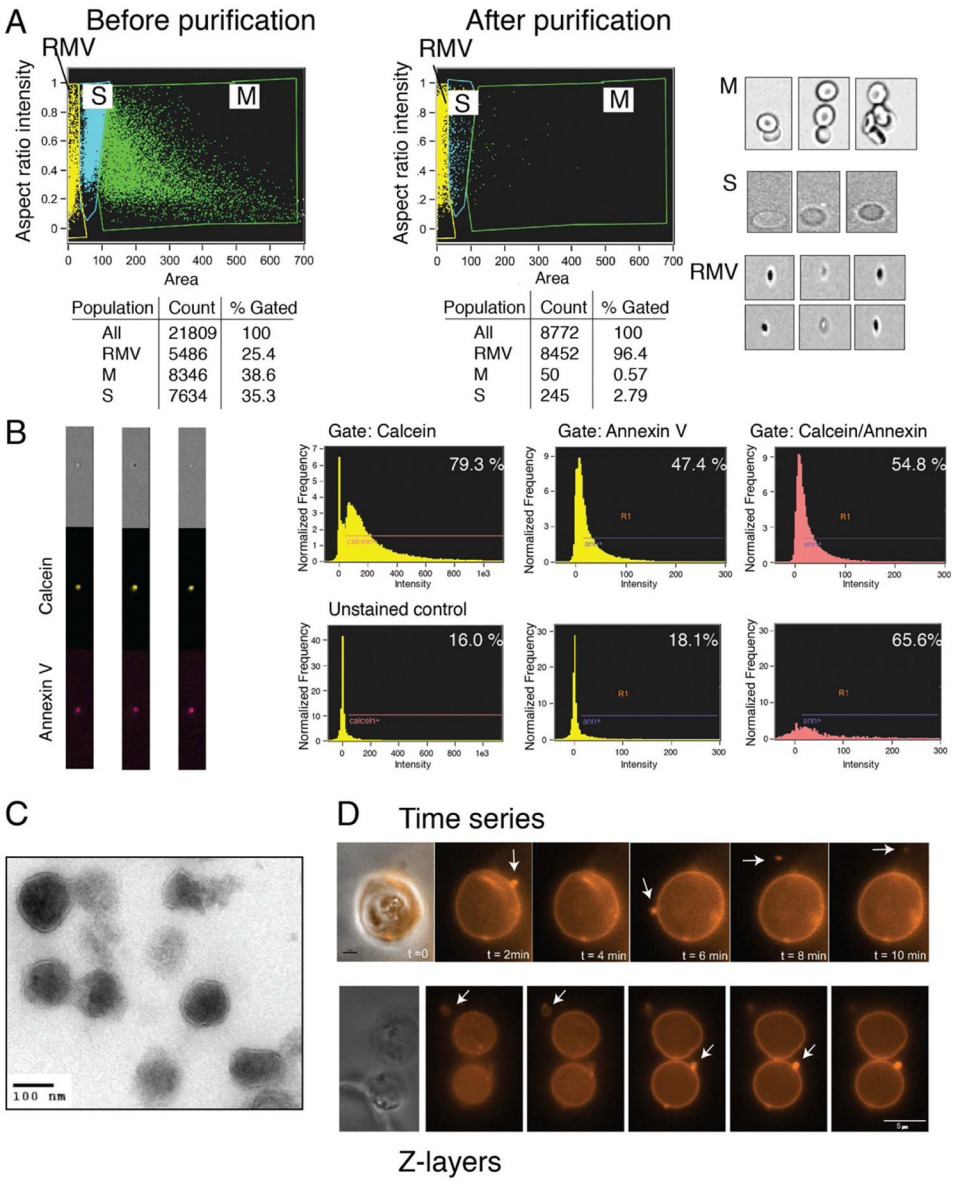

Figure 1. related to Figure S1 and Movies S1. Initial characterization of RMVs from *P. falciparum*-infected red blood cells

A. Analysis of events by ImageStream before and after RMV purification. Non-fractionated cell suspension from *in vitro* culture was analyzed and three populations (S, M and RMV) were differentiated based on intensity and area. Image analysis demonstrates that M consists of clusters of multiple RBCs ("rosettes"), S consists of single RBCs and RMV consists of smaller events of vesicular nature. The RMV purification protocol resulted in an enrichment to > 95% of all events in the RMV gate. **B. Calcein and annexin V labeling of RMVs.** ImageStream analysis of calcein-AM and annexin V antibody staining demonstrates double labeling of RMVs (left panel). By flow cytometry approximately 55% of all events are double positive, although the real number is likely higher due to the limited sensitivity and size cut-off of flow cytometry (right panel). **C. Characterization of the RMV population by electron microscopy.** Analysis of fixed RMVs from *P. falciparum in vitro* cultures reveals vesicular structures of 100 – 400 nm. **D. Live imaging of RMV release.**

Release was captured by time-lapse microscopy of infected RBCs labeled with the surface marker CellVue, using 2-minute intervals over the course of 2 hours (top panel). Serial images were taken across the z-plane by fluorescence microscopy of individual cells (bottom panel). In both cases multiple RMVs can be observed emerging from a single infected RBC.

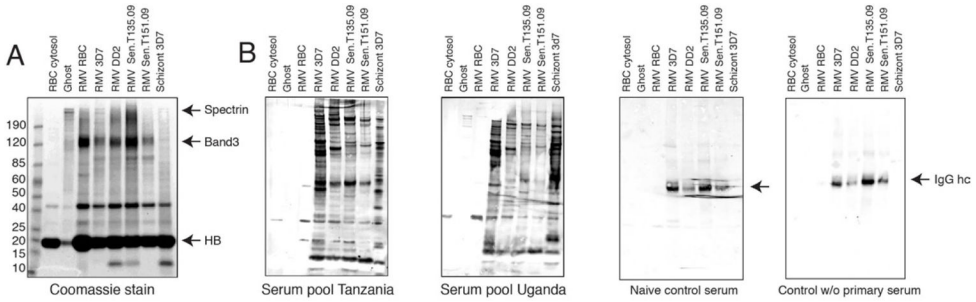

Figure 2. Detection of parasite antigens in RMVs from iRBCs

A. Commassie Blue staining. RMV samples from four parasite strains, as well as control samples from parasite schizont stage lysate, RBC ghosts and RBC cytosol are analyzed. Shown are RMV and control samples, normalized by protein content, and 15 μg loaded onto a 4–12% SDS-PAGE gel per lane before Commassie staining. Note the partial or complete depletion of spectrin in RMV samples, while hemoglobin (HB) appears equally present across all samples. Unique bands are present in RMVs from iRBCs. **B. Detection of parasite antigens by immunoblotting.** Pooled serum from 20 malaria-infected individuals from Mbola, Tanzania (left panel) and Ruhiira, Uganda (right panel) was used for detection of parasite antigens. Multiple high molecular weight bands can be observed in the RMV samples that are absent from whole schizont lysates. Controls include serum from naïve individuals and immunoblot without primary antibody (serum). In both cases only IgG is detected. HB: Hemoglobin.

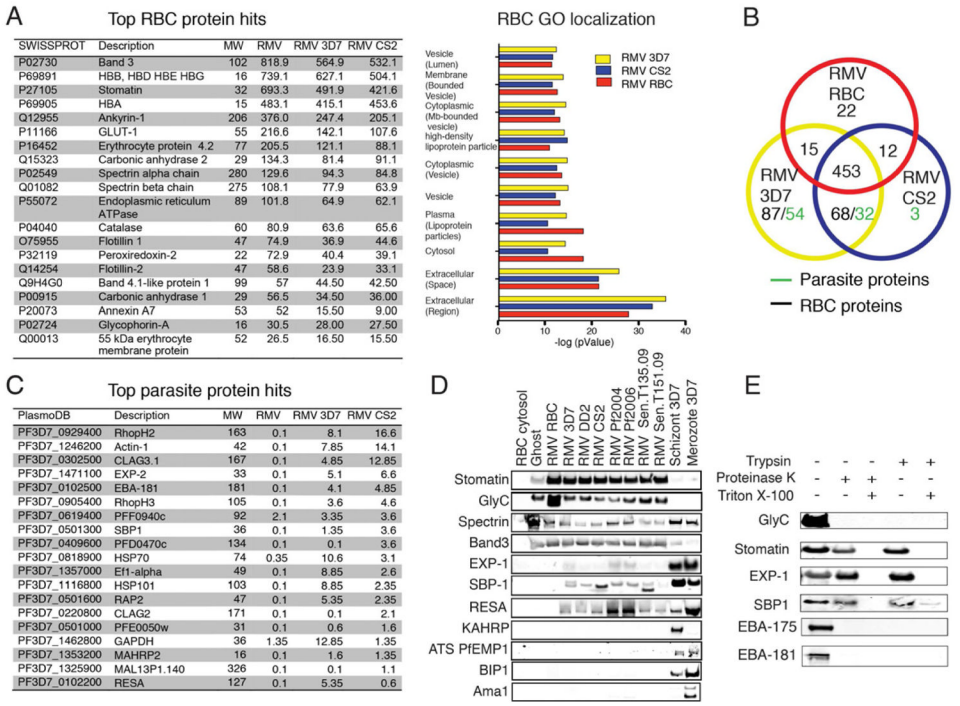

SWISSPROT	Description	MW	RMV	RMV 3D7	RMV CS2
P02730	Band 3	102	818.9	564.9	532.1
P69891	HBB, HBD HBE HBG	16	739.1	627.1	504.1
P27105	Stomatin	32	693.3	491.9	421.6
P69905	HBA	15	483.1	415.1	453.6
Q12955	Ankyrin-1	206	376.0	247.4	205.1
P11166	GLUT-1	55	216.6	142.1	107.6
P16452	Erythrocyte protein 4.2	77	205.5	121.1	88.1
Q15323	Carbonic anhydrase 2	29	134.3	81.4	91.1
P02549	Spectrin alpha chain	280	129.6	94.3	84.8
Q01082	Spectrin beta chain	275	108.1	77.9	63.9
P55072	Endoplasmic reticulum ATPase	89	101.8	64.9	62.1
P04040	Catalase	60	80.9	63.6	65.6
O75955	Flotillin 1	47	74.9	36.9	44.6
P32119	Peroxiredoxin-2	22	72.9	40.4	39.1
Q14254	Flotillin-2	47	58.6	23.9	33.1
Q9H4G0	Band 4.1-like protein 1	99	57	44.50	42.50
P00915	Carbonic anhydrase 1	29	56.5	34.50	36.00
P20073	Annexin A7	53	52	15.50	9.00
P02724	Glycophorin-A	16	30.5	28.00	27.50
Q00013	55 kDa erythrocyte membrane protein	52	26.5	16.50	15.50

PlasmoDB	Description	MW	RMV	RMV 3D7	RMV CS2
PF3D7_0929400	RhopH2	163	0.1	8.1	16.6
PF3D7_1246200	Actin-1	42	0.1	7.85	14.1
PF3D7_0302500	CLAG3.1	167	0.1	4.85	12.85
PF3D7_1471100	EXP-2	33	0.1	5.1	6.6
PF3D7_0102500	EBA-181	181	0.1	4.1	4.85
PF3D7_0905400	RhopH3	105	0.1	3.6	4.6
PF3D7_0619400	PFF0940c	92	2.1	3.35	3.6
PF3D7_0501300	SBP1	36	0.1	1.35	3.6
PF3D7_0409600	PFD0470c	134	0.1	0.1	3.6
PF3D7_0818900	HSP70	74	0.35	10.6	3.1
PF3D7_1357000	Ef1-alpha	49	0.1	8.85	2.6
PF3D7_1116800	HSP101	103	0.1	8.85	2.35
PF3D7_0501600	RAP2	47	0.1	5.35	2.35
PF3D7_0220800	CLAG2	171	0.1	0.1	2.1
PF3D7_0501000	PFE0050w	31	0.1	0.6	1.6
PF3D7_1462800	GAPDH	36	1.35	12.85	1.35
PF3D7_1353200	MAHRP2	16	0.1	1.6	1.35
PF3D7_1325900	MAL13P1.140	326	0.1	0.1	1.1
PF3D7_0102200	RESA	127	0.1	5.35	0.6

Figure 3. related to Figure S1 and Table S1. Compositional analysis of RMVs by proteomic profiling and immunoblotting

A. Most abundant RBC proteins as estimated by peptide counts. Left: The top 20 RBC proteins are ranked by peptide counts detected in RMVs from uRBCs (labeled RMV). These are compared with peptide counts in RMVs from iRBCs (parasite strains 3D7 or CS2). Apart from hemoglobin, the most abundant RBC proteins in all three samples are band 3 and stomatin. Right: Representation of all RBC protein hits identified after stratification by GO term enrichment analysis for cellular localization (additional graphs are available in Figure S2). **B. Protein composition in the 3 samples analyzed.** A Venn diagram representing total RBC and parasite proteins identified in the 3 samples is shown. Proteomics experiments are representative of 2 biological replicates performed in technical duplicates. **C. Most abundant parasite proteins as estimated from peptide counts.** Shown are the top 20 parasite proteins ranked by peptide counts that were identified in RMVs derived from iRBCs, from both parasite strains analyzed. Among the most abundant proteins are parasite invasion ligands (EBA-175, EBA-181) and RBC membrane-associated proteins (e.g., RhopH2/3, EXP-2, CLAG3.2, RESA, SBP1, MAHRP). **D. Confirmation of RMV proteins by immunoblotting.** RMVs are analyzed for the presence of parasite and host proteins that were identified by proteomic analysis. 4 RBC and 7 parasite markers are tested. These are the RBC membrane markers stomatin, glycophorin C and spectrin; the secreted parasite proteins Exp-1 (parasitophorous vacuole membrane and Maurer's clefts), SPB1 (Maurer's clefts), KAHRP (knobs on the iRBC surface), PfEMP1 (knobs on the iRBC surface) and RESA (RBC cytoskeleton and membrane), as well as the merozoite surface protein AMA1 and the parasite marker BIP (parasite ER). Glycophorin C appears to be reduced in RMVs from iRBCs; spectrin is reduced while stomatin is enriched in all RMVs compared to RBC ghosts. The same controls and parasite strains are analyzed as in Figure 3. Loading was normalized by using 8 μg of protein for each lane. **E. Distribution of RBC and parasite proteins in RMVs using enzyme protection assays and immunoblotting.** Four integral membrane proteins are analyzed: the two RBC surface proteins glycophorin C and stomatin, as well as the 2 parasite proteins SBP1 and Exp-1. We also investigated the localization of

the 2 invasion ligands EBA-181 and EBA-175 to determine whether they peripherally associate with RMVs upon shedding during invasion. To test localization of these proteins, RMVs were treated with proteinase K or trypsin in the presence or absence of TX-100. By western blot analysis, glycophorin C as well as EBA-181 and EBA-175 are sensitive to enzyme treatment in the absence of the detergent TX-100, while the other 3 proteins are protected and therefore likely present within internal MV membranes.

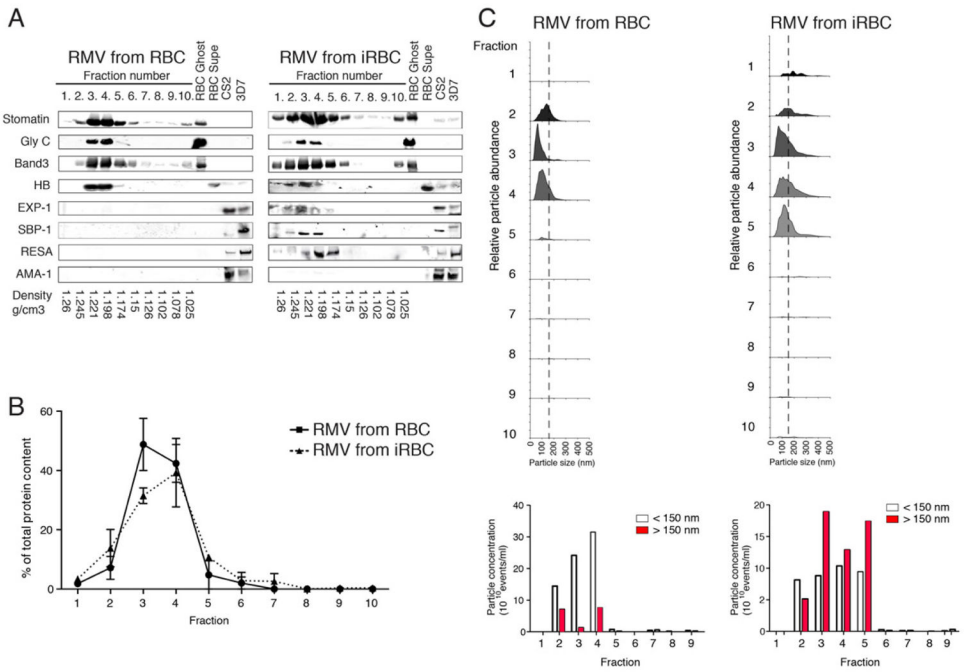

Figure 4. Fractionation of RMVs on a linear sucrose gradient and subsequent analysis

RMVs were prepared as described in Figure S1A and loaded onto a linear sucrose gradient. For all analyses, equal volume of each fraction was analyzed, using fractions from uRBCs and iRBCs. **A. Analysis of fractions by Western blot.** The control samples include RBC ghosts, RBC supernatant and lysates from the 2 reference strains 3D7 and CS2. Membranes were probed with antibodies against stomatin, glycophorin C and band3, as well as Exp-1, SPB1, RESA and AMA-1. Hemoglobin (HB) was detected directly on the Coomassie gel. RMV markers peak in fractions 3 and 4, representing sucrose density between 1.22 (fraction 3) and 1.198 g/cm^3 (fraction 4). AMA-1 is only detected in the parasite lysates but not in any sucrose fraction, suggesting that the RMV preparation that was loaded onto the gradient is not contaminated with merozoites. **B. Analysis of fractions for protein content by BCA.** RMVs showed a peak of protein content in fractions 3 and 4, suggesting that the populations were of homogenous density. Data are presented as mean ±SEM of three independent experiments. **C. Analysis of size and quantity by NanoSight.** Each sample was analyzed using the NanoSight technology to determine size distribution and relative quantity. RMV numbers peak in fractions 3 to 5, and those from infected RBCs contain an additional subpopulation of larger vesicles at 200 to 400 nm size.

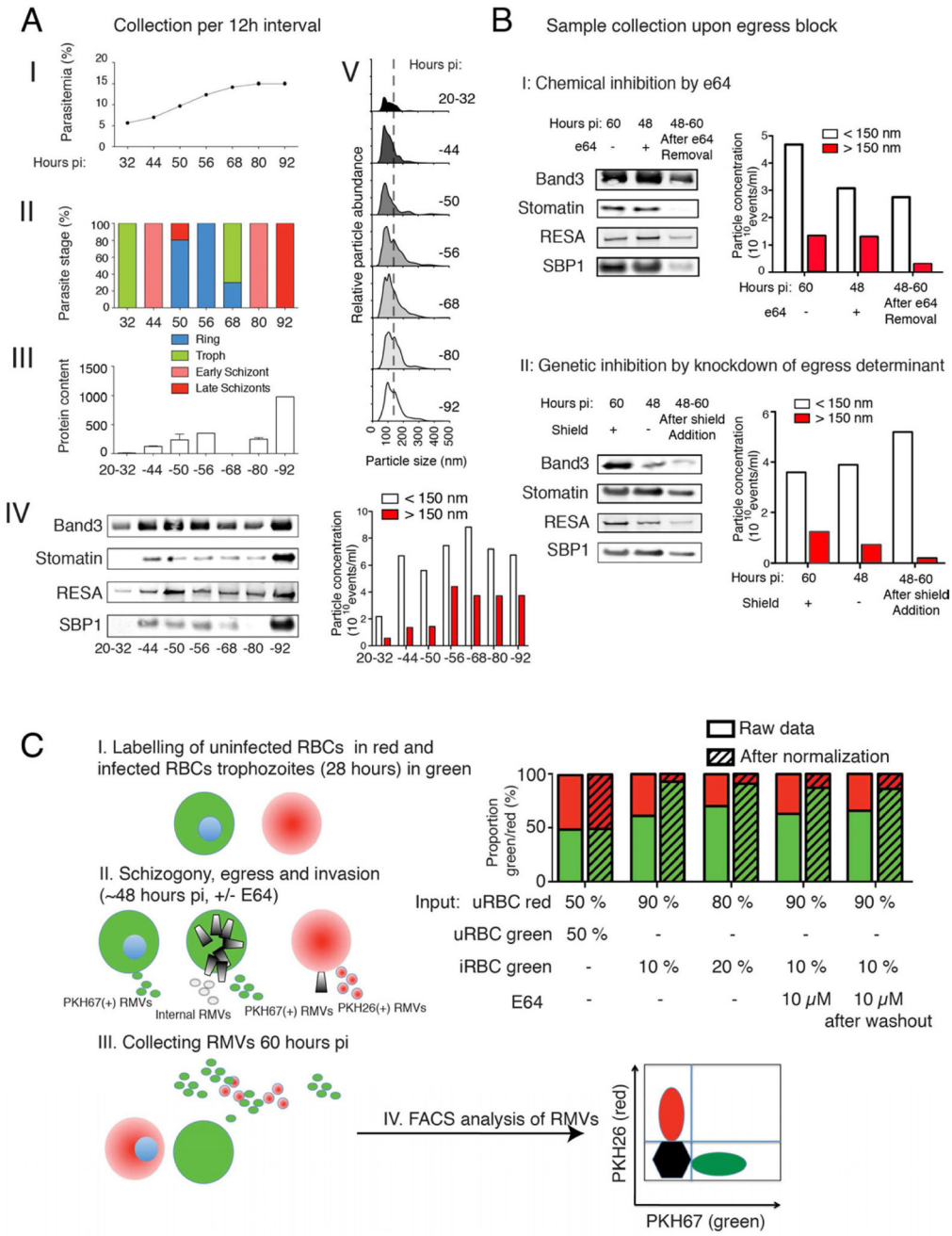

Figure 5. related to Figure S3. Dynamics of RMV release during the asexual RBC cycle of *P. falciparum*

A. Analysis by collection of sample after incubation for time intervals. Highly synchronized parasite cultures (parasite strain 3D7) were initiated at low parasitemia and grown for varying hours post invasion (pi). RMV release was measured in specific time intervals by changing the medium at the beginning of the interval. At collection, parasite pellets were collected to determine parasitemia (I) and parasite stage distribution (II). Supernatant was collected for purification of RMVs and further analysis by BCA (III), western blot (IV) and Nanosight (V). The data demonstrate that the biggest increase in protein content (BCA) and RMV formation (Nanosight) coincides with late schizont stages

(parasitemia). This also coincides with the peak in levels of RMV markers stomatin, band3, RESA and SBP1 in schizont stages. **B. Genetic and chemical inhibition of egress to determine time point of RMV release.** To determine whether the majority of RMVs is released before or during egress we blocked this process chemically by e64 or using a conditional knock-down strategy. **I. Inhibition by the cysteine protease inhibitor e64.** Addition of e64 does not inhibit RMV formation, as determined by Western blot probing for band3, stomatin, RESA and SBP1, and by NanoSight. **II. Inhibition using genetic knock-down of CDPK5.** Quantification of RMV formation after inhibition of egress by knock-down of CDPK5 function (Dvorin et al., 2010). Removal of shield in CDPK5-DD parasites does not reduce RMV formation, as measured by Western blot probing for the same markers as in the e64 experiment and by NanoSight**. C. PKH labeling to determine the relative contribution of RMVs from iRBCs to total RMV production during *in vitro* culture.** The set up of this experiment is represented in subpanels I-IV. I. Synchronized iRBCs (28h pi) are isolated by Percoll gradient, labelled with PKH67 (green) and mixed at different proportions (either 1/10 or 1/5) with uRBCs that have been labeled with PKH26 (red). II/III. After another invasion round (60h pi) supernatant is collected and RMVs purified. A subset of cells are incubated with e64 before egress and until 60h pi, or for 12h after which the compound is washed out and cells further cultured until 60h pi. IV. Red and green RMVs are quantified by flow cytometry. Shown are proportions as measured by flow cytometry, or after normalizing for the proportion of input cells (i.e., proportion of green iRBC *versus* uRBCs). After normalization, an approximately 10-fold excess of RMVs from iRBCs over those from uRBCs is consistently observed.

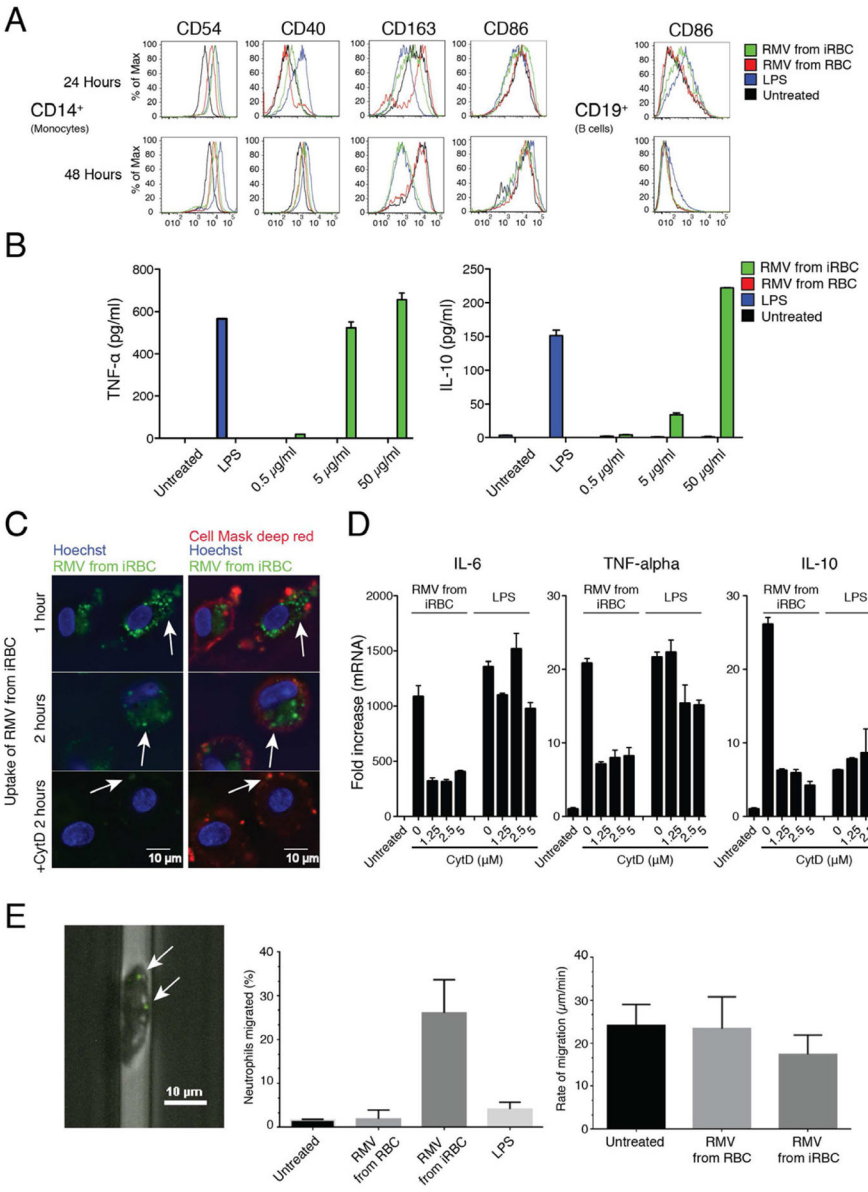

Figure 6. related to Figure S4. Immune stimulatory activity of RMVs

A. Activation of PBMCs. Quantification of activation markers per cell type by flow cytometry. Multiple markers are up-regulated in monocytes as well as CD86 in B cells. **B. Activation of macrophages.** TNF-α and IL-10 production by stimulated macrophages was measured by performing ELISA on the supernatant. Data are presented as mean ±SD and are representative of three independent experiments. **C. RMV uptake into human macrophages.** Human macrophages were stimulated for 1 or 2 h with RMV isolated from iRBC culture supernatants in the presence or absence of cytochalasin D (2.5 μM); cell membranes were stained with fluorescent Cell Mask Deep Red (red) and nuclei were stained with Hoechst 33342 dye (blue), followed by analysis of PKH67-labeled RMV uptake (green). Scale bars, 10 μm. Multiple internalized green vesicles can be observed in the absence of CytD, while RMVs are only present on the macrophage surface upon CytD treatment (white arrows). **D. Inhibition of macrophage RMV phagocytosis.** IL-6, TNF-α and IL-10 transcription by macrophages stimulated with RMVs from iRBCs and uRBCs in

the presence or absence of cytochalasin D was assessed by real-time PCR. Data are presented as mean ±SD and are representative of three independent experiments. **E. Neutrophil activation by RMVs.** Pre-incubation of neutrophils with RMVs from iRBCs shows strong activation, while LPS and RMVs from uRBCs have a minor effect (left panel). Neutrophils activated by RMVs from iRBCs have a reduced migration rate compared to those from uRBCs and untreated controls (right panel). RMVs attached to a neutrophil incubated in the device are shown in the image on the left. White arrows show PKH67-labeled RMVs. Data are presented as mean ±SD and are representative of three independent experiments.

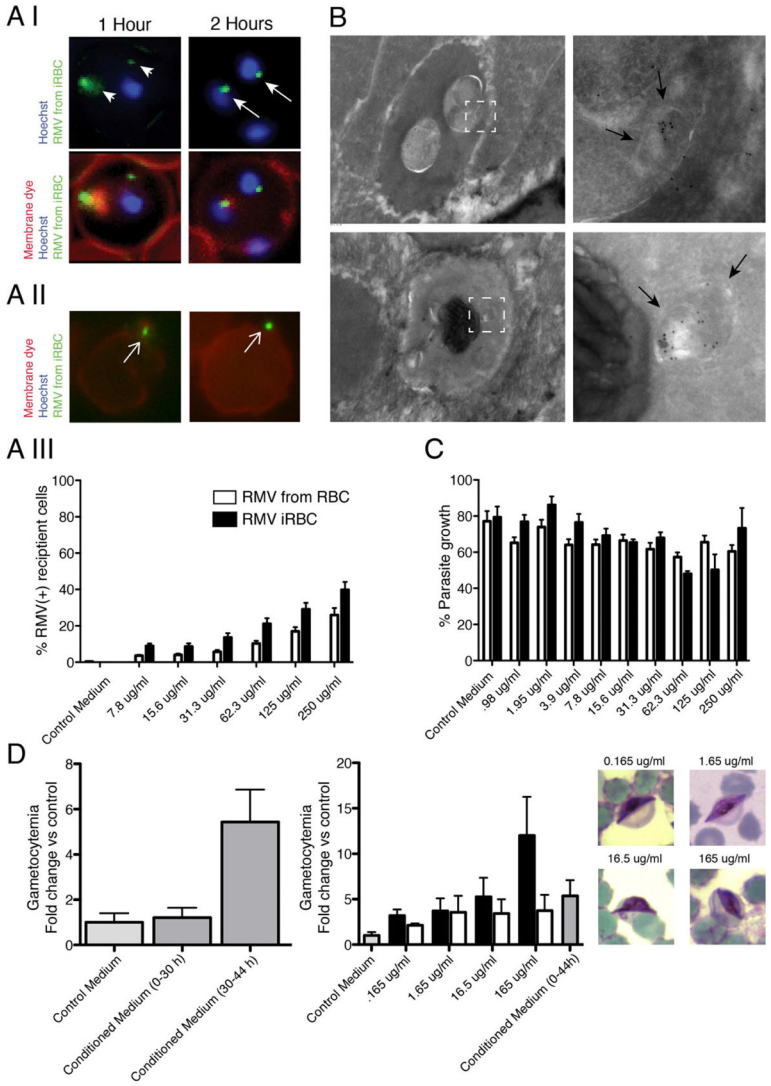

Figure 7. related to Figure S5. RMV uptake and gametocyte production

A. Live analysis of RMV internalization into RBCs. PKH67 labeled RMVs are incubated with RBCs and uptake into live cells is analyzed after 1 and 2 hours incubation by fluorescence microscopy (panels I and II) or flow cytometry (panel III). Uptake into infected RBCs can readily be detected as vesicular structures accumulate in the host cell and at the parasite periphery after 1 hour of incubation, and in a perinuclear location after 2 hours (white arrows). Flow cytometry data are presented as mean ±SD of four independent experiments. **B. Ultrastructural analysis of RMV internalization.** Biotinylated RMVs are incubated with RBCs for 24 hours and prepared for immunogold labeling. Labeled vesicles are detectable in the parasite, within larger membrane structures (black arrows), suggesting that they have not been internalized by endocytosis-like membrane fusion events. **C/D. RMV Effect on parasite growth and gametocyte formation.** No significant alteration of parasite growth is detectable after one replication cycle (C). Data are presented as mean ±SD of four independent experiments. Incubation of infected RBCs with RMVs derived from infected RBCs increases gametocyte formation in a dose-dependent manner (D). Likewise conditioned medium from late stage parasites but not from early stage parasites stimulates

gametocyte formation. Data are presented as mean ±SEM of three independent experiments. Representative gametocytes captured at the time point of readout are shown.